

# Hydrogen tunneling in biology

Amnon Kohen and Judith P Klinman

The mechanistic details of hydrogen transfer in biological systems are not fully understood. The traditional approach has been to use semiclassical transition-state theory. This theory cannot explain many experimental findings, however, so different approaches that emphasize the importance of quantum mechanics and dynamic effects should also be considered.

Address: Departments of Chemistry and Molecular and Cell Biology, University of California at Berkeley, Berkeley CA 94720, USA.

Correspondence: Judith P Klinman  
E-mail: klinman@socrates.berkeley.edu

**Chemistry & Biology** July 1999, **6**:R191–R198  
<http://biomednet.com/elecref/10745521006R0191>

© Elsevier Science Ltd ISSN 1074-5521

## Hydrogen transfer

Hydrogen transfer is of great general importance to many processes in biology, ranging from proton transfer across membranes to the numerous functional isomerizations of intermediary metabolites, and the transfer of reducing equivalents between substrates and cofactors. The increasing evidence for quantum effects in enzyme catalyzed hydrogen-transfer processes leads to a reassessment and expansion of the conceptual framework that underlies enzyme catalysis.

## Conventional theory

Most textbooks and fundamental literature treat enzyme-catalyzed reactions, including hydrogen transfer, in terms of transition-state theory (TST) [1,2]. TST assumes that the reaction coordinate may be described by a single free energy minimum and a single maximum defining the reactant well and the barrier for activation, respectively (Figure 1). The distribution of states between the ground state (GS, the minimum)  $[X]$ , and the transition state (TS, at the top of the barrier)  $[X^\ddagger]$ , is assumed to be an equilibrium process that can be estimated by the Boltzmann distribution:

$$[X^\ddagger] = [X] \exp\left(\frac{-\Delta G^\ddagger}{kT}\right) \quad (1)$$

where  $\Delta G^\ddagger$  is the free energy difference between GS and TS,  $T$  is the absolute temperature and  $k$  is the Boltzmann constant. Classical physics shows that a particle at the top of a barrier can go to product at a frequency ( $\nu$ ) of about  $6 \times 10^{12} \text{ s}^{-1}$  at  $25^\circ\text{C}$ . The reaction rate is given by:

$$\frac{-d[X]}{dt} = \nu[X^\ddagger] = \nu[X] \exp\left(\frac{-\Delta G^\ddagger}{kT}\right) \quad (2)$$

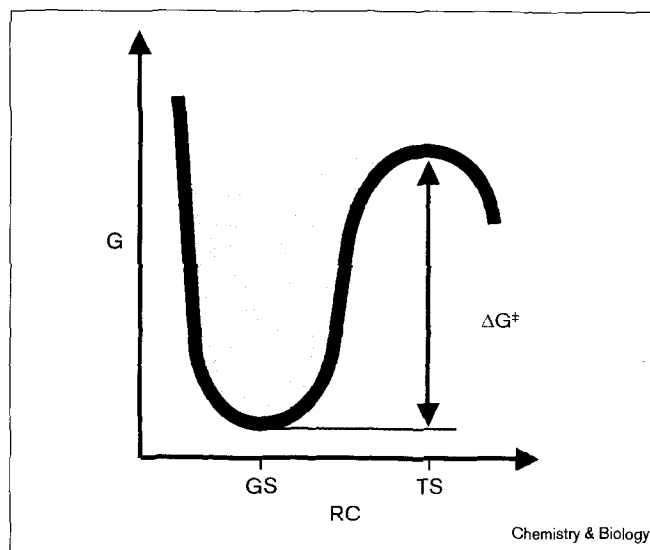
This leads to the Arrhenius equation:

$$\ln(k) = \ln(A) - \frac{\Delta E_a}{RT} \quad (3)$$

where  $A$  is the Arrhenius pre-exponential factor,  $\Delta E_a$  is the activation energy and  $R$  is the gas constant.

The importance of equations 2 and 3, and of TST in general, is that they relate the rate of a reaction to an energy barrier. Notably, only the height of the activation barrier plays a role in determining the reaction rate, regardless of the shape of the potential surface. TST requires that all degrees of freedom in the system are in thermal equilibrium at the TS. This static, thermodynamic approach can

Figure 1



A one-dimensional potential surface where the reaction coordinate (RC) is the distance between the nuclei and  $G$  is the free energy of the system. GS, ground state; TS, transition state.

explain much about reaction rates and catalysis. It has led to the widely accepted notion that catalysts work by stabilizing the TS relative to the ground state, and, in effect, decrease  $\Delta G^\ddagger$  [1]. This concept has resulted in the development of catalytic antibodies raised from TS analog haptens, the design of drugs that resemble the putative TS and give rise to tight binding inhibition, as well as numerous other advances in chemistry and biology.

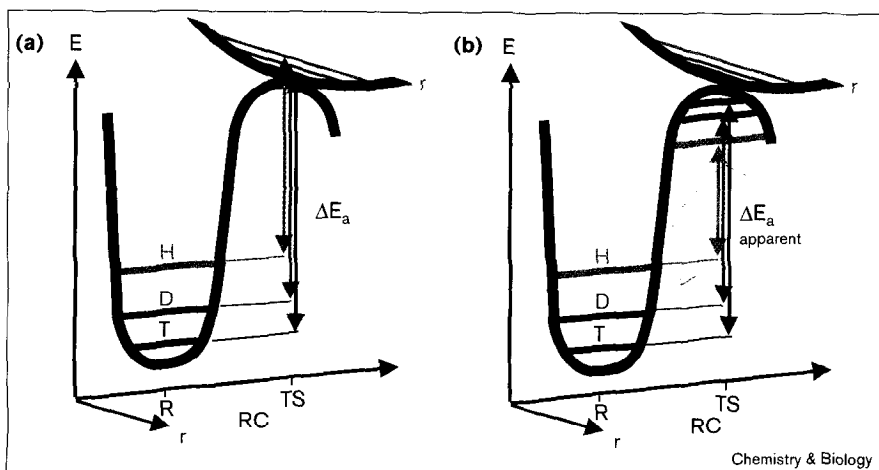
A major problem in characterizing the chemical TS of an enzymatic reaction is that enzymatic transformations take place within multistep kinetic cascades. Measurements of

steady-state kinetics or even pre-steady-state kinetics do not normally indicate which microscopic steps are being studied. For many systems it is the formation or decomposition of the reactive complex step that has the major effect on the experimental measurement. The use of kinetic isotope effects (KIEs) is one of the most powerful methods available to isolate the bond-cleavage steps from nonisotopic binding/release steps and protein conformational changes [3]. KIEs are the ratio of reaction rates for two isotopes and reflect the movement of particles of different mass along the same electronic potential surface. The hydrogen KIE is particularly useful because the mass ratio of its isotopes is much larger than that of any other element, resulting in relatively large KIEs [4].

#### Semiclassical theory and the tunneling correction

What is the origin of KIEs? Because of the uncertainty principle, the lowest energy level a particle can occupy is always above the electronic potential minimum (denoted as the zero point energy, ZPE). The smaller the particle, the less well defined its location and the higher its ZPE. A major contribution to KIEs is the difference between the ZPEs of GS and TS among the different isotopes (Figure 2a) [4]. Although this semiclassical theory of KIEs invokes a correction to TST, it ignores the uncertainty in the location of the transferred particle along the reaction coordinate close to the TS. The latter factor may be estimated from the particle's de Broglie wavelength  $\lambda = h/(2mE)^{1/2}$ , where  $m$  is the particle's mass and  $E$  is its energy. This wavelength for a hydrogen with an energy of 10 kJ/mol is thereby calculated to be 0.5 Å for  $^1\text{H}$  (protium, H), 0.31 Å for  $^2\text{H}$  (deuterium, D) and 0.25 Å for  $^3\text{H}$  (tritium, T). As the reacting bond climbs the energy barrier, it reaches a position where the wavelength of its particle exceeds the barrier width. At this point product (P) can be formed without having reached the energy of the TS. This quantum mechanical effect is denoted as

Figure 2



(a) The semiclassical model. Different energies of activation ( $\Delta E_a$ ) for protium (blue), deuterium (green) and tritium (red) resulting from their different ZPE at the GS and TS.

The GS-ZPE is constituted by all degrees of freedom but mostly the ZPE stretching frequency along the reaction coordinate (RC). The TS-ZPE is constituted by all degrees of freedom orthogonal to the reaction coordinate ( $r$ ). R, reaction well; TS, transition state.

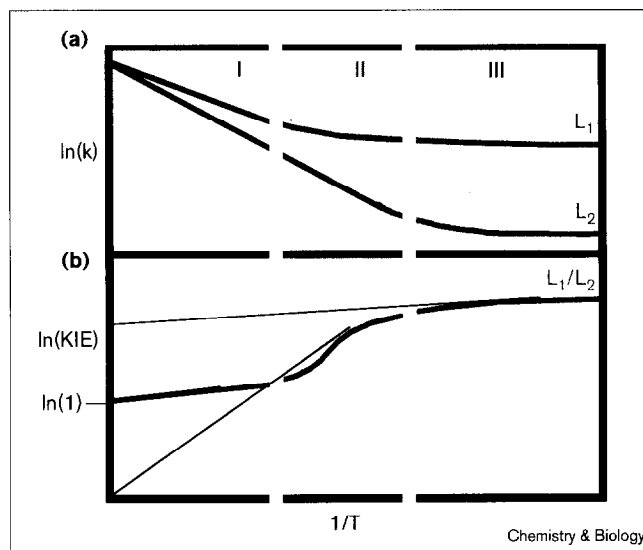
(b) Tunneling correction for a TST type of model. In addition to its higher ZPE, the lighter isotope tunnels at a lower energy under the top of the barrier, resulting in smaller  $\Delta E_a$  (relative to that of heavier isotopes) than predicted by the semiclassical model.

tunneling because the particle seems to ‘dig a tunnel through the barrier’ and the system actually never has to reach the TS. Figure 2b demonstrates how this increases the reaction rate for H more than for D and T and thereby increases the KIEs. Traditional theories that include this effect in their rate and KIE calculations add a correction to TST, and the most widely used formalism is the Bell correction for a parabolic barrier [5]. At very high temperature, as excess thermal energy is available, this effect is negligible and the temperature dependence of the reaction presents a linear behavior on an Arrhenius plot ( $\ln(k)$  versus  $1/T$ ; e.g. Figure 3a, no tunneling region). At very low temperatures, the contribution of thermal activation is lost and only tunneling contributes to the reaction rate. As the tunneling rate is temperature independent, the Arrhenius plot in this region is flat (e.g. Figure 3a, extensive tunneling region). Between these two extremes the plot curves upwards as its slope changes from  $-\Delta E_a/R$  to zero (e.g. Figure 3, moderate tunneling contribution). As a lighter particle is more affected by tunneling than its heavier isotope, this curvature takes place at a higher temperature (lower  $1/T$ ) for the light isotope. Consequently, the KIE temperature dependence will vary, as illustrated in Figure 3b.

### Experimental probes

The models presented in Figures 2 and 3 indicate several experimental approaches for probing tunneling. For the majority of experimental systems only a narrow temperature range is accessible, and plots of  $\ln(\text{KIEs})$  versus  $1/T$  appear linear (Figure 3). The temperature dependence of KIEs in region II, however, will be steeper than at the high-temperature classical region and the dependence in region III will be more shallow. Consequently, nonclassically large or small  $\Delta\Delta E_a/R$  on the KIE Arrhenius plots can indicate tunneling (Figure 3b) [5]. The ‘apparent’ isotopic ratio of Arrhenius pre-exponential factors ( $A_1/A_2$ ), which are the intercepts of the tangents to the plot in Figure 3b at any experimental temperature, are especially sensitive to tunneling. They are close to unity for classical hydrogen transfer, have inverse values under conditions of moderate tunneling and become significantly greater than one in the extensive tunneling region [6]. In general, a KIE larger than the semiclassical limit can indicate a tunneling contribution, but should not be considered a definitive indicator unless other mechanisms capable of inflating observed KIE are eliminated [7]. As an alternative to deviations from semiclassical Arrhenius behavior, multiple KIEs (i.e. a comparison of  $k_H/k_T$  with  $k_D/k_T$ ) can provide direct evidence for tunneling. An exponential relationship is defined relating the two KIEs as  $k_H/k_T = (k_D/k_T)^{\text{exponent}}$ . Semiclassically, this exponent value is close to 3.3, with moderate tunneling capable of inflating this value as high as 15 [8–11]. The basis of this methodology is that tritium serves as an internal reference point, allowing an estimation of the degree of tunneling of protium in relation to

**Figure 3**



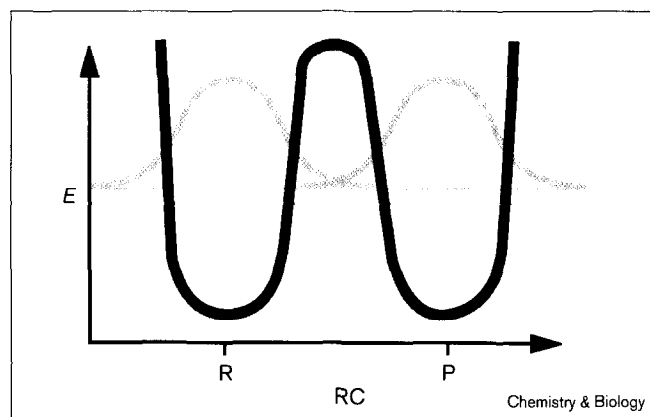
An Arrhenius plot of hydrogen transfer with a temperature-independent tunneling contribution (from absolute zero to infinite temperature). (a) Arrhenius plot of a light isotope ( $L_1$ , blue) and heavier isotope ( $L_2$ , red) over the full temperature range. (b) Arrhenius plot of their KIE ( $L_1/L_2$ , green). Highlighted are experimental temperature ranges for three systems: I, one with no tunneling contribution (yellow background), II, one with a moderate tunneling (grey background) and III, one with extensive tunneling contribution (blue background). The black lines are the tangents to the plot at each region that constitute the experimental fit to the Arrhenius plot.

deuterium. Kinetic complexity decreases the exponent below 3.3, and it should be expected that many observed exponents may reflect a balance between kinetic complexity (exponent  $< 3.3$ ) and quantum behavior (exponent  $> 3.3$ ) [6,12]. These experimental probes have been used both in solution chemistry and in enzymology to estimate the tunneling contribution to reaction rates.

### Vibrationally enhanced tunneling

Many advances have been made in chemistry and biology by using a tunneling approach to correct TST. Experimental data frequently arise that cannot be explained by this approach, however. There are systems with a large energy of activation ( $\Delta E_a$ ), and large KIEs, but no temperature dependence of the KIEs, which are inconsistent with the prediction shown in Figure 3 [13–15]. For other systems, extensive tunneling has been indicated from a small  $\Delta\Delta E_a$ , small values of  $\Delta E_a$  and  $A_1/A_2 > 1$ , but KIEs that are too small to be explained by pure tunneling through a rigid barrier [16]. A number of theoretical approaches have been developed in recent years that attempt to rationalize these data [17–23]. Below we introduce a concept that we believe has the most general application to biologically important systems.

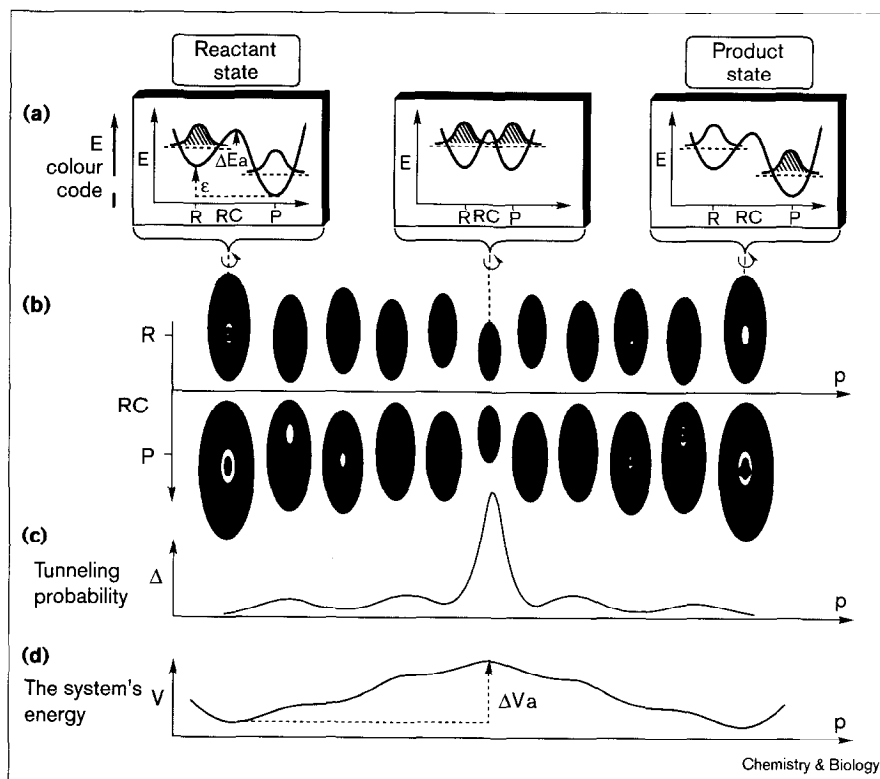
In this model, hydrogen is transferred from one bond state (the reactant state) to the other (the product state) and its

**Figure 4**

An example of ground-state nuclear tunneling along the reaction coordinate (RC). The reactant well (R) is on the left side and product well (P) on the right. The blue line describes the probability functions of a particle. The greater the overlap of the R and P probability functions, the higher is the tunneling probability.

transfer can be discussed in terms of a double-well system. Tunneling is now denoted for a situation in which the probability of finding the particle at the reactant well overlaps under the barrier with the probability of finding it at the product well (Figure 4). The extent of tunneling

between two bound states is a function of the shape of both reactant and product wells, and of the barrier separating them. Tunneling is less affected by the barrier height than by the barrier width and by the degeneracy of the energy levels of reactant and product in the two wells (Figure 4). If the potential surface is rigid, and tunneling takes place between two vibrational ground states of equal energy, the particle will simply tunnel back and forth at the same rate. In order to obtain a net reaction rate, coherency has to be destroyed, which can be achieved by a fluctuation in the system that alters the relative energies of reactant and product. As a minimum, two types of fluctuations will determine the tunneling probability: the first influences the symmetry of the system and the second brings the two wells close enough together for tunneling to occur (Figure 5). The latter is essential because bound substrates are often too far from one another to support tunneling. Theories formalizing such notions for solid-state, solution and enzyme-catalyzed reactions had been published previously [17,19,24–26], and more recently in a series of papers by Antoniou and Schwartz [21–23]. A hydrogen is transferred along a X–H–Y linear system (X and Y are C, O or N) and the environment oscillators (i.e. the enzyme's normal modes) affect the reaction coordinate through asymmetric couplings (which alter the relative energies of the reactant well, R, and the product well, P), as well as a symmetric

**Figure 5**

An illustration of how dynamics can promote hydrogen tunneling. In the course of the system evolving from reactant state to product state the potential surface of the reaction coordinate (RC) is fluctuating due to its coupling to the oscillations of the environment. (a) One-dimensional slices of the potential energy surface. The blue lines are the probability functions at the reactant well (R) and the product well (P). The red areas indicate the occupancy of the probability functions.  $\epsilon$ ; exothermicity of reaction. (b) Energy contours of the potential surface on which the particle (in grey) is being transferred. The distance between reactant to product wells is fluctuating fivefold faster than the symmetry of the double-well system. The plot shows the changes in the RC along one transfer cycle (the  $p$  coordinate). (c) Due to quantum mechanical requirements, the tunneling probability ( $\Delta$ ) is greatest for the more symmetric system with shorter transfer distances. (d) The system's rearrangement energy along the  $p$  coordinate. Theoretical work has shown that the reaction rate and its temperature dependence for such a model are a function of the rearrangement energy ( $\Delta V_a$ ) and the exothermicity of the reaction ( $\epsilon$ ) but not the RC barrier's height ( $\Delta E_a$ ) [22].

coupling (denoted as the tunneling-promoting vibration, which alters the distance between R and P). Figure 5 illustrates this approach on an energy-contour map. The temperature dependence of the KIEs is a function of the degree of coupling of the symmetric vibration to the reaction coordinate, because only the distance between donor and acceptor is sensitive to the isotopic labeling. Such a model is capable of explaining experimental observations that cannot be rationalized using rigid-barrier models.

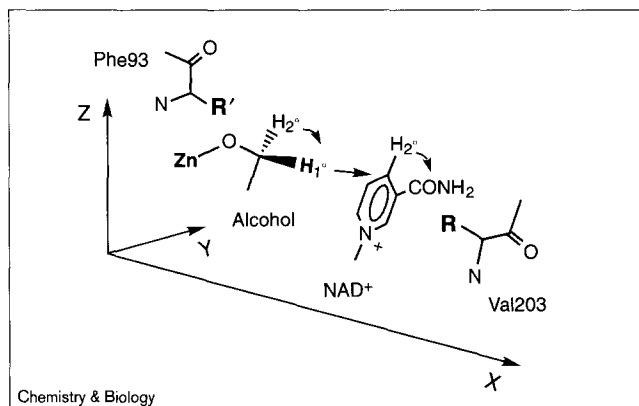
### Implications for enzymology

The implications of the above-described vibrationally enhanced tunneling model for enzyme catalysis are enormous. To promote hydrogen tunneling, an enzyme will have evolved not only to stabilize the TS but to bring donor and acceptor closer together, and to alter the respective energy levels of R and P. The dynamics of the enzyme and the active site are, therefore, expected to be directly involved in the reaction rate enhancement. Altogether, it may be suggested that the role of enzyme dynamics in catalysis is not complete once the reactants are bound in close proximity within a reactive complex. The enzyme may still control and enhance the rate of the chemical step(s) by a coupling of normal modes to the reaction coordinate. In these instances, an average GS conformation may not reveal the actual nature of catalysis.

This last statement deserves further deliberation. The apparent success of TST in explaining biochemical phenomena supported the hope that the knowledge of enzymes structure would result in a complete understanding of their activity. It was presumed that the rigid structure of the active site (preferably in complex with a TS analog) would be sufficient to understand the mechanistic details of the activity. Despite the increasing wealth of structural data, it is still not possible to provide a full qualitative and quantitative framework for catalysis.

The possibility that enzyme dynamics are important to function has not been ignored, and several authors have proposed that enzymes evolved to utilize their inherent fluctuations to affect catalysis [27,28]. It has been recognized that protein flexibility is crucial for the formation of the active complex, namely for substrate binding, product release and also, in some cases, for protein rearrangement. Yet, TST has led to the notion that, once the active complex had been formed, the active site would remain rigid while the barrier involving chemical bond breaking and bond making was being crossed. A few researchers have suggested that enzymes would use dynamics to enhance catalysis in a non-TST manner, but most fall short of supporting this notion with conclusive evidence [29]. The detection of hydrogen tunneling in enzyme reactions, however, compels us to focus our attention on the issues of barrier width and fluctuations.

**Figure 6**



The hydride-transfer step at the HLADH active site (X, Y and Z are Cartesian coordinates). The arrows indicate the motion of the nuclei.  $H_1^\circ$  denotes the transferred hydrogen and  $H_2^\circ$  the secondary hydrogens. Two active site residues (Phe93 and Val203) are also illustrated.

### Experimental examples

Several enzymatic systems in which hydrogen tunneling was initially demonstrated have subsequently been examined with regard to the features discussed above.

#### The correlation between tunneling and barrier width

The actual distance that will affect tunneling is the one between the minima of the donor and acceptor energy wells (Figure 3), and not simply the internuclei distance. A rotational movement that increases the overlap in the molecular orbitals involved in the reaction could decrease the effective barrier width, whereas a shorter distance between nuclei may decrease this overlap [30]. The correlation between tunneling and structure change in an enzyme active site has been addressed in a recent study of mutant forms of horse liver alcohol dehydrogenase (HLADH) [31,32]. The reaction catalyzed by HLADH involves hydride transfer from a primary alcohol to an  $NAD^+$  cofactor (Figure 6). The idea that classical hydride transfer may not explain this enzymatic reaction was first discussed in a theoretical treatment by Huskey and Schowen.[33]. These authors were attempting to reproduce experimentally measured primary ( $1^\circ$ ) and secondary ( $2^\circ$ ) KIEs, in particular  $2^\circ$  KIEs that were larger than the semiclassical limit as defined by the equilibrium isotope effect. Their final model invoked both hydrogen tunneling and coupled motion between the primary and secondary hydrogens. Subsequent studies confirmed that the motion of the transferred hydride ( $1^\circ$ ) is coupled to the concomitant motion of the  $2^\circ$  hydrogens on both the alcohol and the cofactor as they undergo change in their  $\sigma$  bonds hybridization ( $s-sp^3$  to  $s-sp^2$  at the alcohol and  $s-sp^2$  to  $s-sp^3$  at the cofactor) [34].

Figure 6 shows two residues of the HLADH active site that are in contact with bound substrate: Phe93 in the

Table 1

**Kinetic and distance parameters for the hydride transfer catalyzed by mutants of HLADH.**

Parameter	Phe93→Trp	Phe93→Trp Val203→Ala
$k_{\text{cat}}/K_M$ ( $\text{mM}^{-1}\text{s}^{-1}$ )	4.7	0.13
exponent = $\ln(k_H/k_T)/\ln(k_D/k_T)^*$	6.1	3.9
$C4_{(\text{NAD}^+)} \rightarrow C\alpha_{(\text{TFE})}$ (Å)	3.2	3.6 <sup>†</sup>

Both structures are of a ternary enzyme complex with bound  $\text{NAD}^+$  and trifluoro-ethanol (TFE) at a resolution of 2.0 Å [31,32]. \*Exponents relating secondary KIEs [8–10,34,43]. <sup>†</sup>In addition to longer distance from the reacting carbon of the alcohol substrate, the nicotinamide ring has rotated away forming a wider angle between reactants [32].

substrate pocket and Val203 at the back of the nicotinamide ring of cofactor. An increase in the size of R' (Phe93→Trp) has been shown to 'unmask' tunneling, a result of the hydride-transfer event becoming more rate determining [35]. This mutant now serves as a frame of reference for hydrogen tunneling in HLADH catalysis, making it possible to examine the effect of second mutations on the hydrogen-transfer step directly. As summarized in Table 1, a reduction in bulk at position 203 to alanine (smaller R group; Figure 6) is accompanied by a fall off in both catalytic efficiency ( $k_{\text{cat}}/K_M$ ) and tunneling (the size of exponents relating the secondary KIEs for labeled alcohols). X-ray structures of these mutants allowed an estimation of the increase in distance between the reacting carbons as the nicotinamide ring rotates away from the alcohol into the space created by deletion of the methyl groups in position 203 (R changes from an isopropyl to a methyl group) [32].

This is the first example of biological system in which an observed correlation between hydrogen tunneling and the donor–acceptor distance has been detected. Although the observed structural differences could have multiple catalytic consequences, it is reasonable to suggest that the increase in carbon–carbon distance and the distortion of the nicotinamide ring angle induce a significant increase in the reaction barrier width for the double mutant, which manifests itself in reduced tunneling and catalytic efficiency. It is also important to note that, for both the mutant and wild-type forms of HLADH, the structures solved with  $\text{NAD}^+$  and substrate analogs (pentafluorobenzyl alcohol or TFE) indicate a donor–acceptor distance too large to accommodate either tunneling or over-the-barrier hydrogen transfer, with the implication that the distance between nuclei must narrow at the point of hydrogen transfer (see the discussion of enzyme dynamics and tunneling below).

Another set of systems in which barrier width may play a pronounced role is in the enzyme-catalyzed homolysis of C–H bonds with high intrinsic bond dissociation energies.

The adiabatic energy barrier for such cleavages is expected to be difficult to stabilize electrostatically, because the charge distribution at the TS may not differ significantly from the substrate GS. In these instances, hydrogen tunneling would be an excellent solution to rate acceleration, via modulation of the barrier shape. One such system is the reaction catalyzed by lipoxygenase, which shows one of the largest KIEs ever measured in an enzyme system, together with a very small enthalpy of activation ( $\Delta E_a$ ), and almost no difference in enthalpy of activation ( $\Delta\Delta E_a$ ) for C–H and C–D cleavages (Figure 3, region III) [16,36,37]. Recently, two other enzyme systems catalyzing hydrogen-atom abstraction from carbon have also been demonstrated to give abnormally large KIEs: galactose oxidase has a reported  $k_H/k_D$  of 22 at room temperature and inverse  $A_H/A_D$  [38], and methane monooxygenase has a  $k_H/k_D$  close to 100 under single turnover conditions [39].

**Enzyme dynamics and tunneling**

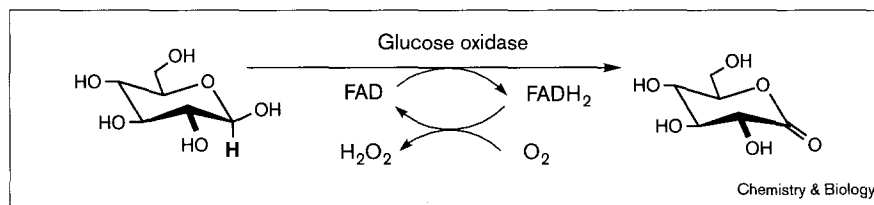
A study with the glycoprotein glucose oxidase (GO) gave the first indication of a correlation between the degree of tunneling and protein rigidity [40]. Different glycoforms of GO were studied for possible tunneling in the reaction in which the anomeric hydrogen at C-1 of glucose is transferred to flavin (Figure 7).

As no secondary hydrogen is present at C-1, the temperature dependence of the KIEs was studied as a probe of tunneling. A correlation was revealed with three glycoforms of the same polypeptide chain in which increased glycosylation had an influence on C–D cleavage. Increased glycosylation was found to decrease the isotope effect on the Arrhenius pre-exponential factors ( $A_D/A_T$ ) from values larger than the semiclassical range to a value smaller than this range. It was suggested that addition of polysaccharides on the surface of the enzyme changed the nature of hydrogen transfer from a region with extensive tunneling to one with only a moderate tunneling contribution (Figure 3). As the closest glycosylation site is 22 Å away from the active site [41], the effect is indirect and the glycosylation must affect the protein in a fashion that is critical to tunneling enhancement. As discussed elsewhere [40,42], there is evidence that surface glycosylation of proteins can induce rigidity [28]. According to the model in Figure 5, the effect of such rigidity in reducing protein fluctuations would be a decrease in the tunneling probability.

An even clearer example of the effect of thermal fluctuations on tunneling in enzyme catalysis comes from a recent study of a thermophilic ADH from *Bacillus stearothermophilus* LLD-R strain (ADH-hT) [15]. ADH-hT shows considerable sequence and structural homology with the previously characterized yeast and horse liver ADHs. Using the competitive methodology described for

Figure 7

The reaction catalyzed by glucose oxidase



HLADH above, the exponents ( $\ln(k_H/k_T)/\ln(k_D/k_T)$ ) were measured over a temperature range of 5–65°C. Additionally, initial rates were measured with protonated and deuterated substrate over the same temperature range. The experimental details and results are described elsewhere [15] and here we summarize only the findings that are relevant to the issue of the role of dynamics in tunneling. For the ADH-hT, a mechanistic phase transition was found around 30°C. Above this temperature, namely in the enzyme's physiological temperature range, the exponents relating secondary  $k_H/k_T$  and  $k_D/k_T > 10$  and the KIEs are mostly temperature independent (within experimental error), resulting in a value of  $A_H/A_D$  larger than unity. All these data are consistent with a significant contribution of tunneling and coupled motion to hydride transfer. In contrast, at lower temperature, the exponents decrease towards the semiclassical limit, the KIEs demonstrate a much steeper temperature dependence and the  $A_H/A_D$  becomes much smaller than unity. Apparently, at reduced temperature, the degree of tunneling is suppressed and the system falls into a moderate tunneling region (see Figure 3). Such a system cannot be understood in terms of a rigid barrier, with or without a tunneling correction. On the other hand, a model of vibrationally enhanced tunneling will explain these findings. The tunneling-promoting vibration is thermally activated, and its fluctuation amplitude will decrease with decreased temperature. At some point below the optimal temperature for ADH-hT, there is insufficient excitation of the tunneling-promoting vibration and the probability of bringing the donor and acceptor close enough together becomes very low. Under these conditions, the rate falls off and the behavior of the system becomes more classical. Contrary to the predictions from studies of small-molecule hydrogen tunneling through rigid barriers, the extent of tunneling with ADH-hT is larger at the elevated temperatures that correspond to its physiologically optimal temperature range.

## Conclusions

The accumulated data indicate a hydrogen-tunneling contribution to many enzymatic reactions involving hydride, proton or hydrogen-radical transfer [6]. For some of these systems a rigid barrier model with a tunneling correction to TST appears sufficient to rationalize the experimental findings, whereas for others a tunneling-promoting vibration

must be invoked. Apparently, neither quantum mechanical effects nor dynamics can be ignored in many enzyme reactions. Development of a more realistic paradigm of enzyme catalysis (and associated hydrogen transfer) requires advances in methodology for the acquisition and interpretation of data regarding protein dynamics and structure in relation to optimal catalysis.

The implications of the ideas discussed here for hydrogen transfer in chemistry and biology are great. Most importantly, they discourage an indiscriminate use of TST in the condensed phase in general and, specifically, in enzymology. Furthermore, attention is drawn to the importance of the entire protein in enzyme catalysis, as protein normal modes may be coupled to the reaction coordinate. These considerations could have significant impact on biomimetic catalyst design. Incorporating the dynamic behavior of a protein, its metastable sub-conformations and low-frequency normal modes, while emphasizing the structural motions that can narrow the activation barrier of the average structure, may provide a missing link between static pictures of enzyme active sites and their activity.

## References

1. Fersht, A. (1998). *Structure and Mechanism in Protein Science*. W.H. Freeman, New York.
2. Kraut, J. (1988). How do enzymes work? *Science* **242**, 533-540.
3. Cook, P.F. (1991). *Enzyme Mechanism from Isotope Effects*. CRC Press, Boca Raton, Florida.
4. Melander, L. & Saunders, W.H. (1987) *Reaction Rates of Isotopic Molecules*. R.E. Krieger, Malabar, Florida.
5. Bell, R.P. (1980). *The Tunneling Effect in Chemistry*. Chapman & Hall, London & New York.
6. Kohen, A. & Klinman, J.P. (1998). Enzyme catalysis: beyond classical paradigms. *Accounts. Chem. Res.* **31**, 397-404.
7. Thibblin, A. & Ahlberg, P. (1989). Reaction branching and extreme kinetic isotope effects in the study of reaction mechanisms. *Chem. Soc. Rev.* **18**, 209-224.
8. Saunders, W.H. (1985). Calculations of isotope effects in elimination reactions. new experimental criteria for tunneling in slow proton transfers. *J. Am. Chem. Soc.* **107**, 164-169.
9. Amin, M., Price, R.C. & Saunders, W.H. (1990). Tunneling in elimination reactions – tests of criteria for tunneling predicted by model calculations. *J. Am. Chem. Soc.* **112**, 4467-4471.
10. Saunders, W.H. (1992). The contribution of tunneling to secondary isotope effects. *Croat. Chem. Acta.* **65**, 505-515.
11. Grant, K.L. & Klinman, J.P. (1992). Exponential relationship among multiple hydrogen isotope effects as probes of hydrogen tunneling. *Bioorg. Chem.* **20**, 1-7.
12. Cha, Y., Murray, C.J. & Klinman, J.P. (1989). Hydrogen tunneling in enzyme reactions. *Science* **243**, 1325-1330.
13. Kwart, H. (1982). Temperature dependence of primary kinetic isotope effect as a mechanistic criterion. *Accounts Chem. Res.* **15**, 401-408.

14. Basran, J., Sutcliffe, M.J. & Scrutton N.S. (1999). Enzymatic H-transfer requires vibration-driven extreme tunneling. *Biochemistry* **38**, 3218-3222.
15. Kohen, A., Cannino, R., Bartolucci, S. & Klinman, J.P. (1999). Thermophilic dehydrogenase: enzyme dynamics role in hydrogen Tunneling. *Nature* **399**, 496-499.
16. Glickman, M.H., Wiseman, J.S. & Klinman, J.P. (1994). Extremely large isotope effects in the soybean lipoxygenase-linoleic acid reaction. *J. Am. Chem. Soc.* **116**, 793-794.
17. Babamov, V.K. & Marcus, R.A. (1981). Dynamics of hydrogen atom and proton transfer reactions. symmetric case. *J. Chem. Phys.* **74**, 1790-1780.
18. Bruno, W.J. & Bialek, W. (1992). Vibrationally enhanced tunneling as a mechanism for enzymatic hydrogen transfer. *Biophys. J.* **63**, 689-699.
19. Borgis, D. & Hynes, J.T. (1993). Dynamical theory of proton tunneling transfer rates in solution – general formulation. *Chem. Phys.* **170**, 315-346.
20. Moiseyev, N., Rucker, J. & Glickman, M.H. (1997). Reduction of ferric iron could drive hydrogen tunneling in lipoxygenase catalysis: implications for enzymatic and chemical mechanisms. *J. Am. Chem. Soc.* **119**, 3853-3860.
21. Antoniou, D. & Schwartz, S.D. (1996). Nonadiabatic effects in a method that combines classical and quantum mechanics. *J. Chem. Phys.* **104**, 3526-3530.
22. Antoniou, D. & Schwartz, S.D. (1997). Large KIE in enzymatic proton transfer and the role of substrate oscillations. *Proc. Natl Acad. Sci. USA* **94**, 12360-12365.
23. Antoniou, D. & Schwartz, S.D. (1998). Activated chemistry in the presence of a strongly symmetrically coupled vibration. *J. Chem. Phys.* **108**, 3620-3625.
24. Borgis, D. & Hines, J.T. (1989). Proton transfer reaction. In *The Enzyme Catalysis Process*. (Cooper, A., Houben, J. & Chien, L., eds), pp 293-303, Plenum, New York.
25. Borgis, D.C., Lee, S.Y. & Hynes, J.T. (1989). A dynamical theory of nonadiabatic proton and hydrogen atom transfer reaction rates in solution. *Chem. Phys. Lett.* **162**, 19-26.
26. Borgis, D. & Hynes, J.T. (1991). Molecular-dynamics simulation for a model nonadiabatic proton transfer reaction in solution. *J. Chem. Phys.* **94**, 3619-3628.
27. Rasmussen, B.F., Stock, A.M., Ringe, D. & Petsko, G.A. (1992). Crystalline ribonuclease-a loses function below the dynamical transition at 220K. *Nature* **357**, 423-424.
28. Rudd, P.M., *et al.*, & Dwek, R.A. (1994). Glycoforms modify the dynamic stability and functional activity of an enzyme. *Biochemistry* **33**, 17-22.
29. Gregory, R.B. (1995). *Protein-Solvent Interactions*. Marcel Dekker, Inc., New York.
30. Mesecar, A.D., Stoddard, B.L. & Koshland, D.E. (1997). Orbital steering in the catalytic power of enzymes: small structural changes with large catalytic consequences. *Science* **277**, 202-206.
31. Bahnson, B.J., Colby, T.D., Chin, J.K., Goldstein, B.M. & Klinman, J.P. (1997). A link between protein structure and enzyme catalyzed hydrogen tunneling. *Proc. Natl Acad. Sci. USA* **94**, 12797-12802.
32. Colby, T.D., Bahnson, B.J., Chin, J.K., Klinman, J.P. & Goldstein, B.M. (1998). Active site modifications in a double mutant of liver alcohol dehydrogenase: structural studies of two enzyme-ligand complexes. *Biochemistry* **37**, 9295-9304.
33. Huskey, W.P. & Schowen, R.L. (1983). Reaction-coordinate tunnelling in hydride transfer reactions. *J. Am. Chem. Soc.* **105**, 5704-5706.
34. Rucker, J. & Klinman, J.P. (1999). Computational study of tunneling and coupled motion. *J. Am. Chem. Soc.*, **121**, 1997-2006.
35. Bahnson, B.J., Park, D.H., Kim, K., Plapp, B.V. & Klinman, J.P. (1993). Unmasking of hydrogen tunneling in the horse liver alcohol dehydrogenase reaction by site-directed mutagenesis. *Biochemistry* **32**, 5503-5507.
36. Glickman, M.H. & Klinman, J.P. (1996). Lipoxygenase reaction mechanism – demonstration that hydrogen abstraction from substrate precedes dioxygen binding during catalytic turnover. *Biochemistry* **35**, 12882-12892.
37. Jonsson, T., Glickman, M.H., Sun, S.J. & Klinman, J.P. (1996). Experimental evidence for extensive tunneling of hydrogen in the lipoxygenase reaction – implications for enzyme catalysis. *J. Am. Chem. Soc.* **118**, 10319-10320.
38. Whittaker, M.M., Ballou, D.P. & Whittaker, J.W. (1998). Kinetic isotope effects as probes of the mechanism of galactose oxidase. *Biochemistry* **37**, 8426-8436.
39. Nesheim, J.C. & Lipscomb, J.D. (1996). Large kinetic isotope effects in methane oxidation catalyzed by methane monooxygenase: evidence for C-H bond cleavage in a reaction cycle intermediate. *Biochemistry* **35**, 10240-10247.
40. Kohen, A., Jonsson, T. & Klinman, P.J. (1997). Effect of protein glycosylation on catalysis: changes in hydrogen tunneling and enthalpy of activation in the glucose oxidase reaction. *Biochemistry* **36**, 2603-2611.
41. Hecht, H.J., Kalisz, H.M., Hendle, J., Schmid, R.D. & Schomburg, D. (1993). Crystal structure of glucose oxidase from *Aspergillus Niger* refined at 2.3 Å resolution. *J. Mol. Biol.* **229**, 153-172.
42. Kohen, A., Jonsson, T. & Klinman, P.J. (1997). Effect of enzyme glycosylation on the chemical step of catalysis, as probed by hydrogen tunneling and enthalpy of activation. In *Techniques in Protein Chemistry VIII* (Marshak, D.R. ed.), pp 311-319, Academic Press, San Diego, New York.
43. Lin, S. & Saunders, W.H. (1994). Tunneling in elimination reactions – structural effects on the secondary beta-tritium isotope effect. *J. Am. Chem. Soc.* **116**, 6107-6110.